Temperature-Controlled Antimicrobial Release from Poly(diethylene glycol methylether methacrylate)-Functionalized Bottleneck-Structured Porous Silicon for the Inhibition of Bacterial Growth

Stephanie Müller, Alex Cavallaro, Krasimir Vasilev, Nicolas H. Voelcker,* Holger Schönherr*

Bacterial infections in wounds slow down the healing process and lead to increased morbidity in affected patients. Polymer coatings on porous membranes were investigated, which facilitate the in situ detection and treatment of, e.g., *Escherichia coli* and *Staphylococcus aureus* infections. The theranostic approach relies on the thermoresponsive polymer poly(diethylene glycol methylether methacrylate) (PDEGMA). The increase of the wound temperature due to infection is targeted in this proof of concept study for triggering the release of the fluorescent antibiotic levofloxacin from bottle-shaped porous silicon (pSi) membranes capped with PDEGMA brushes. Below their lower critical solution temperature (LCST) the PDEGMA brushes are expanded and the levofloxacin release is significantly retarded. By contrast, above the LCST the PDEGMA brushes collapse and levofloxacin is released rapidly, which is detectable in solution owing to its fluorescence properties. The concomitant inhibition of bacterial growth agrees favorably with the drug release determined by fluorescence spectroscopy.

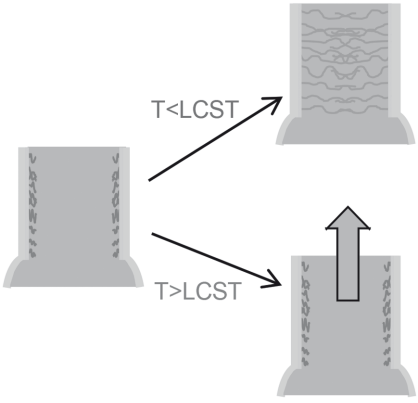

S. Müller, Prof. H. Schönherr
Physical Chemistry I
Department of Chemistry and Biology & Research Center of Micro and Nanochemistry and Engineering (Cμ)
University of Siegen
Adolf-Reichwein-Str. 2, 57076 Siegen, Germany
E-mail: schoenherr@chemie.uni-siegen.de
Dr. A. Cavallaro, Prof. K. Vasilev
School of Engineering
University of South Australia
Mawson Lakes, SA 5095, Australia
Prof. N. H. Voelcker
Future Industries Institute
University of South Australia
Mawson Lakes Boulevard, 5095 Adelaide, Australia
E-mail: nico.voelcker@unisa.edu.au

1. Introduction

Since chronic wounds heal with a dramatically slower rate than acute wounds, infection caused by bacteria is one major problem during the healing process.[1] Even if a wound is covered by an appropriate wound dressing, bacterial infections cannot be avoided in the long term. Both for traditional detection of bacterial infection by swabbing and subsequent microbiology cell culture and for modern methods, wound dressing removal is typically necessary.[2] However, it is painful and may further delay the healing process.[3] To circumvent the time consuming sampling and culturing for the detection of bacterial infections, the development of new biosensors, which can be

Macromol. Chem. Phys. **2016**, DOI: 10.1002/macp.201600099

incorporated into the wound dressing and report the presence of bacteria in situ, is an attractive objective. In situ sensing of pathogenic bacteria can be achieved for instance by detection of characteristic enzymes secreted by these pathogenic bacteria, e.g., via the incorporation of tailor-made enzyme-labile reporter nanocapsules or signaling polymersomes into the wound dressing, which release an incorporated indicator dye upon degradation, or alternatively by autonomously infection reporting hydrogel layers that are equipped with chromogenic or fluorogenic substrates.[4] Another promising approach is based on nanoporous anodic aluminum oxide (AAO) membranes, which are coated with an enzyme labile polymer.[5] Upon enzymatic polymer degradation, the effective refractive index of the membrane is altered, as can be analyzed inline by white-light interferometry.[6]

Hybrids of polymers and silicon-based nanoporous membranes have also been studied in the context of drug release.[7] Reduced pore diameters by plasma deposition of poly(allylamine) were shown to result in retarded release.[8] Alternatively, a coating of a chitosan hydrogel on top of porous silicon (pSi) was shown to function as a pH-responsive valve for the release of insulin that is incorporated in the pores.[9] Recently, McInnes et al. capped the top of pSi by initiated chemical vapor deposition with a thin layer of pH responsive copolymer to control the release of the topoisomerase inhibitor camptothecin.[10] Similarly, Klok and co-workers controlled the flux of Na_2HPO_4/citrate buffer across a carboxylic acid-post-modified poly(2-hydroxyethyl methacrylate) (PHEMA)-grafted AAO membrane via switching the pH (high flux at pH 3, low flux at pH 8).[11] Finally, nanoporous silicon nitride films and membranes were functionalized with poly(methacrylic acid) by Vancso and co-workers to study the pH dependent gating via atomic force microscopy (AFM), current–voltage measurements (to determine the ion conductivity) and by diffusion of Rhodamine 6G through the membrane.[12]

A promising alternative approach for the detection of bacterial infections is the established significant temperature increase in the wound, which is an indirect, but very local indicator for a bacterial infection.[13] A temperature increase may be in general exploited by triggering the opening (or closing) of a thermoresponsive pore, which can be accomplished by applying thermoresponsive polymers like the widely used poly(*N*-isopropyl acrylamide) (PNIPAM) on nanopores for triggering the release of signaling molecules.[14] Zapotoczny and co-workers functionalized AAO platforms with different pore diameters with PNIPAM and performed a pulsatile release of calcein by switching the temperature above and below the lower critical solution temperature (LCST).[15] However, the biocompatibility of PNIPAM is subject to intense debate in the literature, which motivates the search for replacements.[16] For instance, thermoresponsive poly(di(ethylene glycol) methylether methacrylate) (PDEGMA) is known in this context as a nontoxic, biocompatible, and protein-resistant polymer, which fulfills the pre-requirements for the application alluded to above.[17] Desseaux and Klok utilized PDEGMA brushes modified with the tripeptide arginine-glycine-aspartic acid (Arg-Gly-Asp, RGD) to study the nonspecific adhesion of 3T3 cells, which was controlled via switching the temperature to expose or bury the peptides.[18] The LCST of PDEGMA grafted from surfaces has been reported to be higher than the LCST in the bulk (26 °C).[19] More recent studies in our laboratory confirmed that the collapse of PDEGMA brushes grafted from gold surfaces occurs over a wide range of temperatures and exhibits a marked brush thickness dependence. Wassel showed in detailed surface plasmon resonance measurements that the surface transition temperature (determined via the nonreversible adsorption of the protein bovine serum albumin) increases approximately linearly with increasing brush thickness.[20,21] Previously, it was shown that the LCST can be tuned from 26 to 90 °C by synthesizing copolymer brushes of di(ethylene glycol) methylether methacrylate (DEGMA)/oligo(ethylene glycol) methylether methacrylate (OEGMA).[19,22] Exploiting this insight, Vasani et al. studied the release of levofloxacin from PDEGMA/poly(oligo(ethylene glycol) methylether methacrylate (POEGMA)-functionalized biosilica over time and

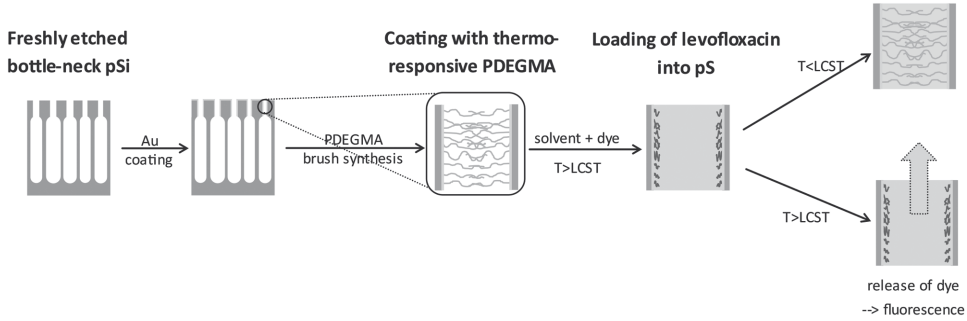

Figure 1. Scheme of functionalization of botteneck-shaped pSi with PDEGMA, loading of the antimicrobial fluorescent dye levofloxacin into the pores above the LCST and thermally stimulated release.

Macromol. Chem. Phys. **2016**, DOI: 10.1002/macp.201600099

observed that the release below the LCST (determined by cloud point measurements to be 36 °C) was significantly slower than above the LCST.[23] Also the burst release was less prominent below the LCST (30% of the drug at T = 25 °C compared to 60% at T = 45 °C). By zone of inhibition bacteria tests, they proved that the drugs were still active after performing the release experiments.

To achieve an opening and closing of the pores only at the pore mouth, pSi was coated in the study reported here with a thin gold coating, which serves to further narrow pore diameter and also as a coating for the functionalization with polymer brushes by surface initiated polymerization from an immobilized initiator. At temperatures above the LCST, the polymer chains are collapsed and the open pore diameter is increased. This collapse effectively eliminates the barrier afforded by the swollen polymer at T < LCST and hence results in a faster diffusion of the enclosed antimicrobial dye from the pores into the medium (Figure 1). The inhibition of bacteria like *E. coli* and *S. aureus* hence can in principle be tuned to temperatures that are found for locally infected wounds. Thus, as reported here, the thermally stimulated release of the antibiotic levofloxacin as a model antimicrobial, which is active against both Gram-positive and Gram-negative bacteria,[24] from a pSi reservoir was studied for different polymer brush thicknesses, release times, and temperatures.

2. Experimental Section

2.1. Materials

DEGMA (average M_n = 300 g mol^{-1}, Sigma-Aldrich) and OEGMA (average M_n = 475 g mol^{-1}, Sigma-Aldrich) were purified via filtration over aluminum oxide under argon pressure. 3-aminopropyl triethoxysilane (APTES, Sigma-Aldrich), 2,2′-bipyridine (bipy, Sigma-Aldrich), cysteamine (Sigma-Aldrich), dichloromethane (DCM Chemsupply), ethanol undenatured (Chemsupply), hydrofluoric acid (HF, 48%, Merck), methanol (Chemsupply), triethylamine (TEA Aldrich), and α-bromoisobutyryl bromide (BiBB, Sigma-Aldrich) were used as received. Copper(I) bromide (CuBr) was synthesized according to the literature.[25]

2.2. Fabrication of pSi Membranes

p++ silicon wafers (Siegert Wafers, resistivity <2 mΩ cm) were etched with varying current densities (25–150 mA cm^{-2}) to obtain straight and bottle-shaped pores in pSi samples in a 3:1 HF:EtOH (vol:vol) solution. Prior to the final etch, a sacrificial etch was performed to remove contaminations and prepattern the silicon surface. The pre-etch was performed at 50 mA cm^{-2} for 30 s and removed in 0.5 M aqueous sodium hydroxide solution. The bottleneck layer was etched for 30 s at a current density of 25 mA cm^{-2}; the layer with the larger pore diameter for 120 s at 150 mA cm^{-2}. For stabilization in aqueous medium, the pSi was thermally oxidized at 800 °C for 1 h and was allowed to cool down to room temperature. The pore size was determined by field-emission-scanning electron microscopy (FE-SEM, Quanta 450 field emission gun environmental SEM, with a solid state secondary ion detector, accelerating voltage: 30 keV).

2.3. Functionalization of pSi with PDEGMA

The pSi membranes (bottle-shaped pores) were functionalized only at the bottleneck part or straight pores with constant diameter were modified with a thermoresponsive coating nominally along the entire membrane. For the functionalization of bottleneck part only, the pSi samples were first sputter-coated with Cr (3 nm) and Au (7 nm). Afterward, the gold-coated pSi was functionalized with cysteamine (8.6 mg per 100 mL in ethanol) overnight. For a complete functionalization of straight pores with constant diameter, APTES was attached via chemical vapor deposition on pSi without prior Au coating.[26] Both cysteamine and APTES introduce an amino-functionality on gold and silicon, respectively. The initiator BiBB (250 µL, 2 mmol; in 5 mL DCM) was linked to the amine-functional pSi via dropwise addition to a solution of dry DCM (30 mL) and TEA (500 µL). After initiator attachment, the surface was rinsed with DCM and ethanol and dried in a clean nitrogen stream. The surface-initiated atom transfer radical polymerization (SI-ATRP) was carried out by transferring the initiator-functionalized samples into a degassed solution of methanol (24 mL), water (6 mL), DEGMA (6.16 mL, 33.4 mmol) or OEGMA (9.54 mL, 33.4 mmol), bipy (624 mg, 4 mmol), and copper(I) bromide (CuBr, 200 mg, 1.4 mmol,) under inert gas atmosphere.[27] The polymerization was stopped by rinsing the samples thoroughly with methanol.

The thickness of the PDEGMA brushes was estimated by measuring the dry thickness on a flat silicon wafer or on a gold-coated silicon sample by ellipsometry (alpha-SE ellipsometer, J. A. Woollam Co., Inc., Lincoln, NE). The samples were measured at three different incidence angles (65, 70, and 75°) with wavelengths between 380 and 900 nm. A two-layer model (1: background; 2: polymer layer) was applied, where the second layer is described by a Cauchy model with a refractive index of 1.45 at a wavelength of 632.8 nm. An initiator-functionalized silicon wafer was used as background.

The functionalized flat silicon and pSi samples were additionally analyzed by X-ray photoelectron spectroscopy (XPS) measurements (S-Probe ESCA SSX-100S, Surface Science Instruments, USA) using Al Kα radiation of 200 W. The spectra were analyzed using Casa XPS processing software version 2.3.16 PR 1.6. The aliphatic C 1s signal (285.0 eV) was used as a reference for calibration of the binding energies.

2.4. Loading of Fluorescent Antibiotic

Levofloxacin was loaded into the pSi membranes by immersing the surfaces in a 10×10^{-3} M solution of the dye in phosphate buffered saline (PBS) at 60 °C for 1 h. Afterward, the samples were dipped three times into Milli-Q water at room temperature, followed by drying in a stream of nitrogen gas.

2.5. Release Study by Fluorescence Spectroscopy

The release of levofloxacin was monitored by fluorescence spectroscopy (Varian Cary Eclipse spectrometer, Varian, Mulgrave, Victoria, Australia). Emission spectra (emission wavelength of 540 nm) were captured using an excitation wavelength of 292 nm with excitation and emission slit width of 2.5 and 5 nm, respectively. The temperature was controlled with a Peltier element. The solutions were stirred with stirring bars inside the cuvettes. The pSi samples were attached to the lid and placed into the PBS solution in the cuvettes. The calibration data (dilution series of levofloxacin in PBS, pH 7.4) were acquired at the applied release temperatures. For the dynamic release experiments, the complete volume of the cuvettes (3.5 mL PBS, pH 7.4) was removed and stored for bacteria tests. The cuvettes were immediately refilled with 3.5 mL of fresh thermostatted PBS solution. The removal and refilling of release solution was repeated every 60 min for 8 h in total.

2.6. Bacteria Tests

The antibacterial activity of levofloxacin released from pSi was assayed against *E. coli* (ATCC 25922) and *S. aureus* (ATCC 29213) in vitro. Bacteria were plated from frozen stocks on nutrient agar plates and incubated at 37 °C. A single bacterial colony was picked and incubated overnight in tryptic soy broth (TSB) at 37 °C. The bacteria were diluted to a concentration of 10^6 CFU mL^{-1} in TSB based on turbidity (OD_{600}). 150 µL of the bacterial suspension and 50 µL of the sample solution were added to each well (96 well plate). 150 µL of uninoculated TSB and 50 µL PBS buffer were used as a blank. The baseline minimal inhibitory concentration (MIC), which is the lowest concentration still inhibiting the growth of bacteria after overnight incubation, was determined by using 16 µg mL^{-1} levofloxacin in PBS solution and diluting this in 1:2 dilution steps (1:1 vol:vol). For the release samples, the number of dilution steps to the MIC was determined. From that the concentration of levofloxacin can be estimated and compared to the concentration determined by fluorescence spectroscopy.

3. Results and Discussion

pSi membranes with a bottle-shaped pores were synthesized by anodization in HF/ethanol. The narrow pore ends afford a maximized pore volume into which the levofloxacin can be loaded. Consequently, in later experiments only the top part of the pSi was functionalized with the thermo-switchable PDEGMA brushes. The initial anodization at a current density of 25 mA cm^{-2} afforded narrow pores, while the subsequent anodization at an increase current density of 150 mA cm^{-2} resulted in wider pores. After oxidation, the pore mouth had a mean pore diameter of 10 nm (Figure S-1, Supporting Information) according to FE-SEM analyses and a length of 1.3 µm (Figure 2). The remainder of the 12.2 µm long pores had a constant mean diameter of 14 nm.

These pSi membranes were first functionalized via chemical vapor deposition of the APTES amino-silane (Figure 3). Subsequently, BiBB was covalently attached by coupling in DCM. Finally polymer brushes were synthesized by the grafting from method by SI-ATRP of DEGMA or OEGMA, respectively. While PDEGMA is known to be thermoresponsive at temperatures close to physiological temperatures,[19] the LCST of POEGMA was reported to be 90 °C. Hence, POEGMA brushes serve as nonthermoresponsive controls of similar chemical composition and properties as PDEGMA.

The polymerization was stopped after specific times to obtain polymer brushes of varying thickness. The dry thickness of brushes synthesized under the conditions stated was determined by ellipsometric measurements on a flat Si wafer (Figure 4). This afforded a nominal thickness value for the functionalized pSi. For short polymerization times (t < 3 h), the dry ellipsometric thickness of PDEGMA on flat Si was found to increase linearly with the polymerization time as expected for SI-ATRP.

The elemental composition of PDEGMA on the pSi surface was analyzed by XPS (Figure 5). In survey scans (Figure S-2a, Supporting Information) the following signals were detected: 532 eV (O 1s), 285 eV (C 1s), 152 eV (Si 2s), 103 eV (Si 2p). In high resolution scans (Figure S-2b,c, Supporting Information) the signals for N 1s and Br 3d were observed at 400.0 and 69.3 eV, respectively. The signal observed

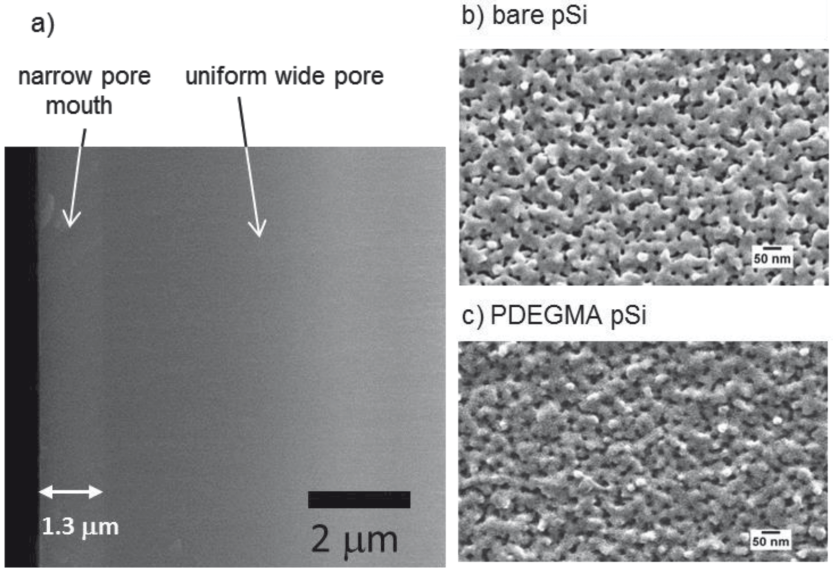

Figure 2. a): Cross-sectional view FE-SEM image of bottle-shaped pSi sample. b,c): Top-view FE-SEM images of Au-coated (for functionalization) pSi: b) bare pSi and c) pSi functionalized with PDEGMA.

Macromol. Chem. Phys. **2016**, DOI: 10.1002/macp.201600099

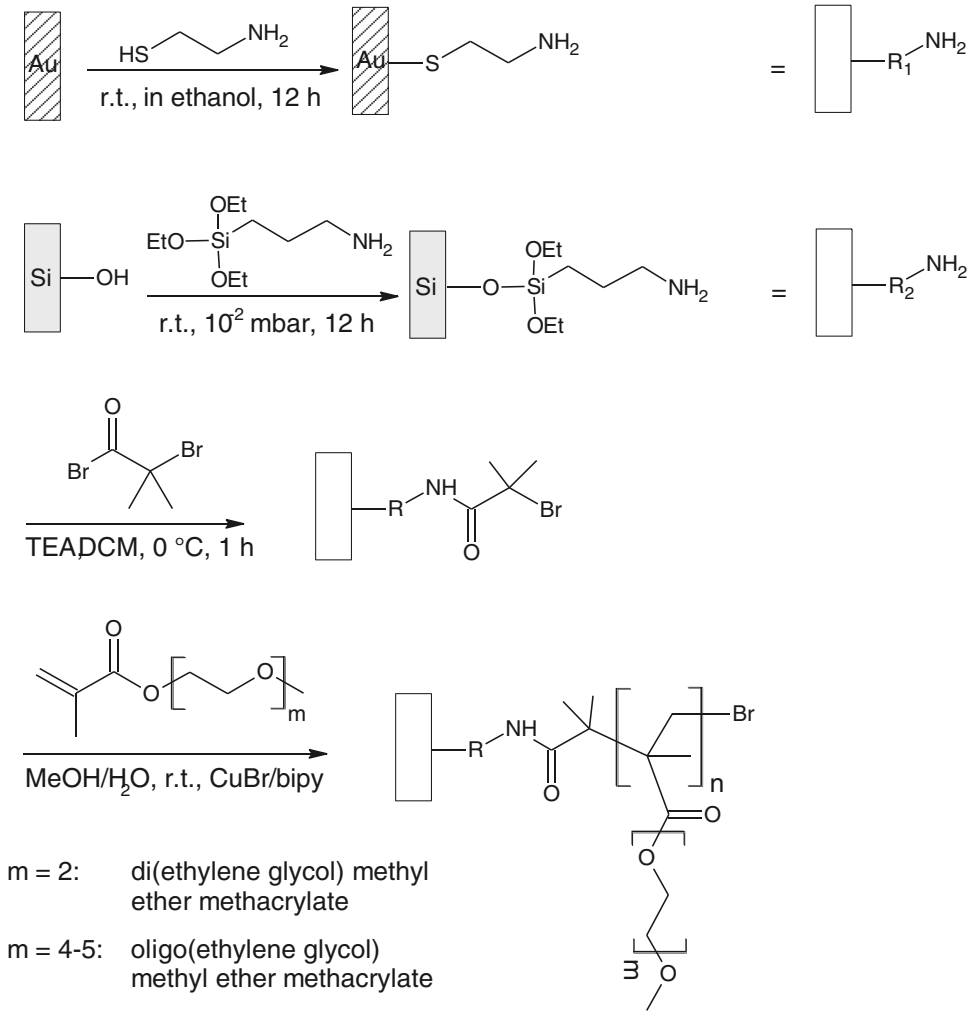

Figure 3. Schematic of functionalization of the pSi substrates by self-assembled monolayer formation on gold-coated or silanized pSi, followed by initiator attachment and SI-ATRP of DEGMA or OEGMA.

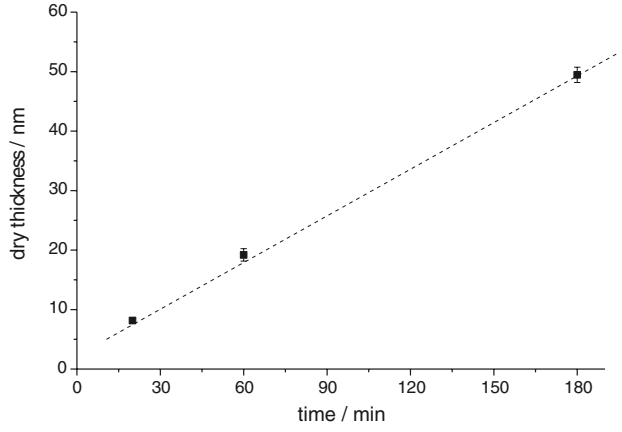

Figure 4. Plot of dry ellipsometric PDEGMA brush thickness versus polymerization time on flat silicon (the thickness of the initiator layer was subtracted). The dotted line represents a linear least squares fit of the data.

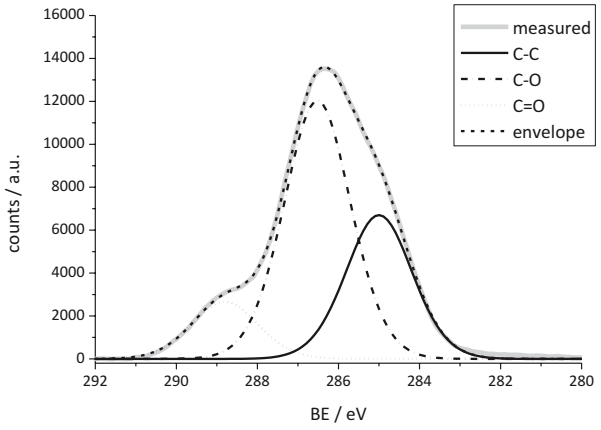

Figure 5. High resolution C 1s XPS spectrum of PDEGMA on pSi. The spectrum was fitted with three components: C—C: 285.0 eV, C—O: 286.5 eV, C=O: 288.8 eV.

in high resolution C 1s scans could be deconvoluted into the following components: C—C: 285.0 eV, C—O: 286.5 eV, C═O: 288.8 eV. The observed ratios of the C 1s carbon peak areas of C—C:C—O:C═O 2.8:5.1:1:1 agree favorably with the theoretical ones: 3:5:1, and are similar to the ratios determined for PDEGMA on flat Si:3.1:4.7:1.2 (Figure S-3, Supporting Information).

In the nanoporous bottle-shaped pores levofloxacin was loaded at a temperature above the LCST of PDEGMA. Encapsulation was afforded by quickly cooling the sample to room temperature during rinsing, which removed the loosely bound antimicrobial dye, followed by drying of the samples. The release experiments were carried out in situ inside a microwell plate, in which the completely immersed substrates were fixed on the side wall. Alternatively, in the dynamic mode, the entire sample solution in a cuvette was exchanged with fresh buffer every 60 min. The concentration of released levofloxacin in a volume of 3.5 mL (2 mL for plate reader experiments) was determined on the basis of a previously recorded calibration curve. The concentration was then converted into the released mass per exposed sample surface area. From these data, the time after which a certain sample would reach the MIC in a defined volume can be estimated.

The dynamic release experiments show a clear and rapid burst release for the initiator-functionalized pSi membranes at high and low temperature (Figure 6). Since the diffusion of levofloxacin out of the pores is not hindered by any polymer coating, the slightly increased release rate at 45 °C compared to 20 °C can be attributed to an increased diffusion coefficient D of levofloxacin according to the Stokes–Einstein equation at higher temperatures due to reduced solvent viscosity ($D \propto \eta^{-1}$) and increased temperature ($D \propto T$). The difference in the plateau values can be attributed to minimal differences in the rinsing and drying step, which would lead to a significant difference for the only initiator-functionalized pSi, where the burst release is not hindered by the PDEGMA brushes. By contrast, the PDEGMA-functionalized membranes exhibit a much slower release of levofloxacin, which is modulated depending on the temperature. At 45 °C (T > LCST) the initial release rate was nine times higher compared to the one at 20 °C, which is below or close to the LCST. The release from POEGMA-functionalized pSi (Figure S-4, Supporting Information) showed a burst release and no significant increase in concentration after 60 min (Figure S-5, Supporting Information) for both temperature conditions. This implies that the faster release observed for PDEGMA-functionalized membranes at T > LCST is caused by the collapse of the polymer brushes and not only caused by faster diffusion due to the increase in temperature. The differences in the release profiles shown in Figure 6 for PDEGMA and in Figure S-5 (Supporting Information) for POEGMA underline that only PDEGMA brushes thermoresponsive in the temperature range of 20–45 °C can modulate the release rate. An increase in polymerization time and concomitantly brush thickness resulted in a slower release at both release temperatures (Figure 6, right). On the contrary, the release of

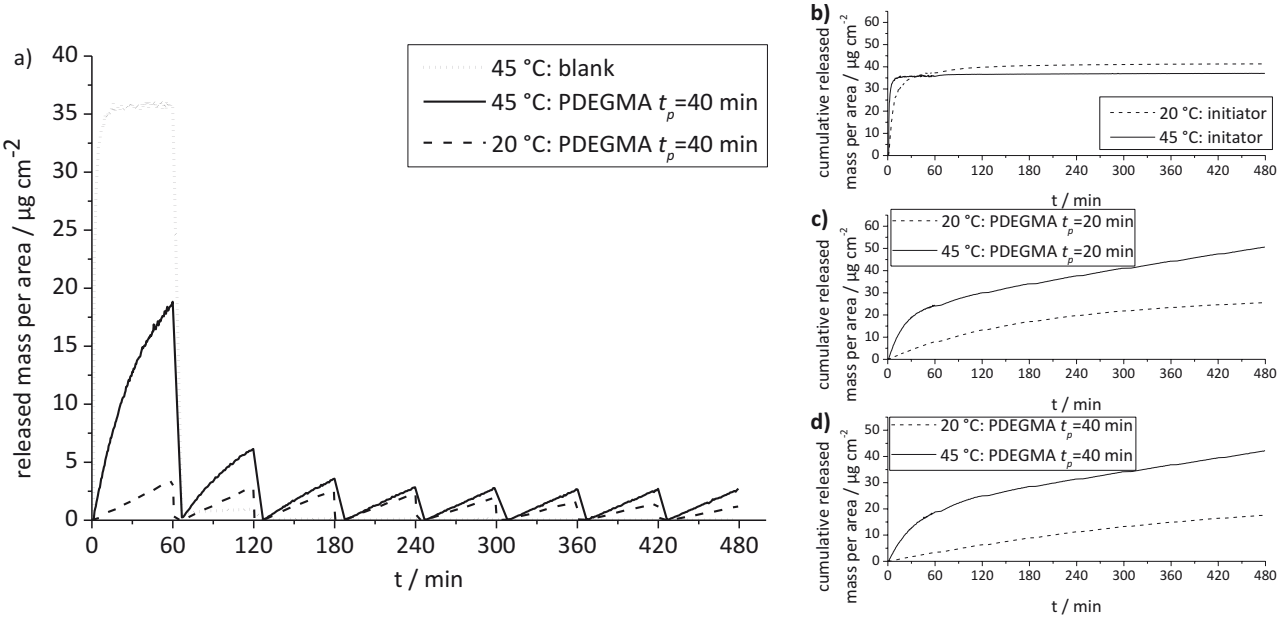

Figure 6. a) Dynamic release curves (exchange of entire cuvette volume with fresh buffer solution every 60 min) of levofloxacin from initiator- and PDEGMA-functionalized pSi (bottle-shaped pores, Au-coated) below and above the LCST. Cumulative released mass per area for the release from b) initiator, c) PDEGMA (20 min polymerization time), and d) PDEGMA (40 min polymerization time) functionalized pSi .

Macromolecular Journals

Macromol. Chem. Phys. **2016**, DOI: 10.1002/macp.201600099

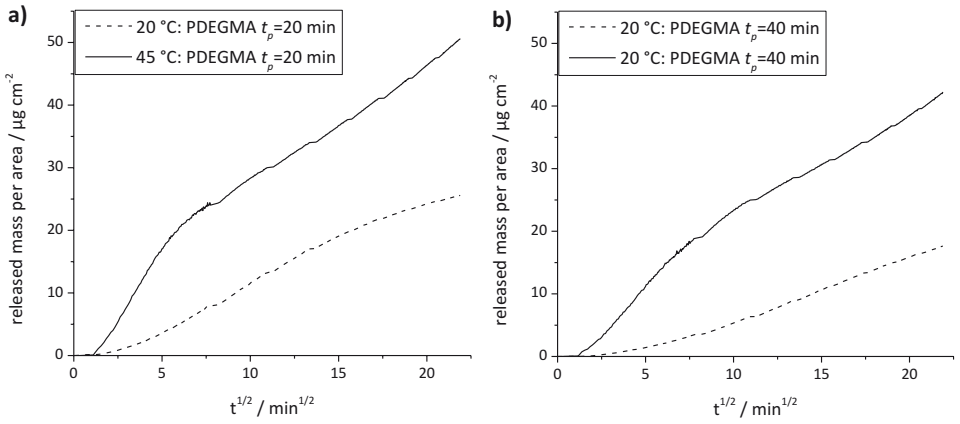

Figure 7. Released mass versus square root of time plots for dynamic release of levofloxacin from pSi membranes (bottle-shaped pores, Au-coated) observed at T < LCST and T > LCST for PDEGMA layers with different thickness. a) Polymerization time 20 min. b) Polymerization time 40 min.

levofloxacin from the initiator-modified pSi (blank experiment) was complete already after 2 h.

Due to the narrow pore opening, we assume that the release is diffusion-controlled. The release data in Figure 6 were fitted against the square root of time (t) (Figure 7 and Figure S-6, Supporting Information), with Q_t being the released mass per area

$$Q_t = k\sqrt{t} \quad (1)$$

The diffusion parameter k depends on the diffusion constant, the initial concentration in the solution (equals zero), the porosity of the matrix system, the drug solubility, and the tortuosity factor (which equals 1 for straight porous systems).[28] Perfect sink conditions are given, if the concentration of the released dye in the medium is negligibly small.[29] Thus, the release of further dye is not slowed down due to a decrease in the concentration gradient. To achieve perfect sink conditions, it is generally recommended that the dye concentration is kept below 10% of the saturation concentration.[30]

The values for the parameter were found to depend on the temperature as well as the thickness of the PDEGMA layer, which was controlled via the polymerization time. However, the release from PDEGMA modifications with varying thickness cannot be compared directly, because the amount of loaded drug was not a priori constant. For comparison of different brush thicknesses, the amount of drug needs to be independently determined, e.g., via thermogravimetric analysis. Also the porosity changes for different temperatures preclude the direct comparison of the release above and below the LCST. Therefore, the ratio of the parameters k was calculated by dividing k obtained by fitting the data for 2–30 min release by k for 1–5 h. The diffusion parameter ratio R_k thus obtained was higher for release above the LCST (for t_p = 20 min: R_k = 2.6, for t_p = 40 min: R_k = 2.0) than for the release below the release (for t_p = 20 min: R_k = 0.7, for t_p = 40 min: R_k = 0.6). This indicates a fast release in the beginning for T > LCST, whereas the initial release at T < LCST is slower.

The fluorescence spectroscopy data shown above allow one to conclude after which time the MIC values were reached. To compare these data to the actual inhibition of bacterial growth due to the released levofloxacin, the number of dilution steps of the samples taken in the dynamic release experiments (complete volume exchange) necessary to reach the MIC were determined. The MIC was determined independently to be 0.03 µg mL^{-1} (determined by dilution series, Figure S-7, Supporting Information)) for *E. coli* (ATCC 25922) and 0.25 µg mL^{-1} for *S. aureus* (ATCC 29213), which agrees with the MICs stated in literature (0.16–0.064 µg mL^{-1} for *E. coli*, 0.125–0.25 µg mL^{-1} for *S. aureus*).[31] The sample solutions taken during the release were diluted 1:4 for the MIC tests to allow the addition of TSB medium for the bacteria. The concentration of levofloxacin in the sample solution after dilution (first sample; calculated from fluorescence spectroscopy data) is shown in Figure 8a. The dilution steps to MIC were determined via 1:2 dilutions of the first sample (Figure 8b). If the dilution steps to MIC are not shown in the graphs, the 1:4 diluted (initial) sample solution did not inhibit the growth of bacteria. For 0, the initial sample inhibited the bacterial growth. After 1 h, all samples (initiator at 45 °C, PDEGMA-functionalized pSi at 20 and 45 °C) exhibited a high enough release to reach the MIC for *E. coli*. After 2 h, the release of levofloxacin from the initiator-functionalized pSi had already decreased to a point where the released antibiotic was not high enough to inhibit the growth of *E. coli*. Alternatively, the PDEGMA-functionalized pSi still released enough levofloxacin to inhibit bacterial growth. This is evident as the number of dilutions required to reach the MIC for these samples were 1 and 2 for 20 and

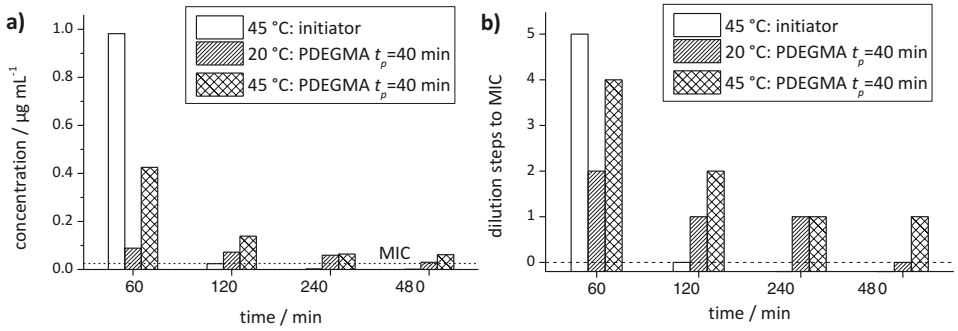

Figure 8. Bacteria tests (*E. coli*): a) Concentration of sample after dilution with medium for samples taken at the timepoints displayed on the *x*-axis (dashed horizontal line: MIC); b) dilution steps to MIC: Dilution steps (1:2) of the released samples for which the bacterial growth was inhibited (for samples, which are not shown, the MIC was not reached).

45 °C, respectively. The level of levofloxacin release from PDEGMA-functionalized pSi at 45 °C, i.e., above the LCST, remained well above the MIC of *E. coli* even after 8 h. In contrast, samples incubated below the LCST released their payload too quickly and could not sustain their release for greater than 4 h. For the inhibition of the growth of *S. aureus* the number of dilution steps to MIC was always smaller (Figure S-8, Supporting Information), because the MIC is higher (0.25 µg mL^{-1}). The growth of *S. aureus* was inhibited only for the first hour of release for the initiator-functionalized pSi at both release temperatures and for the release above the LCST for the PDEGMA-functionalized pSi with a polymerization time of 20 min. From the dilution steps to MIC, the concentration of levofloxacin in the sample solutions can be back calculated (Figure S-9, Supporting Information), which agrees favorably with the concentrations determined by fluorescence spectroscopy during the dynamic release measurements.

As shown by the MIC test, the release of levofloxacin below the LCST is still high enough to inhibit bacterial growth during the first hours of release (for the given sample area and release volume). This can be attributed to the facts that the antimicrobial is present in significant amount in the pore-blocking swollen PDEGMA and that the lower release temperature (20 °C) is close to the temperature, where the collapse of PDEGMA brushes starts.[20] To address this problem, a lower grafting density or copolymers can be applied. By decreasing the grafting density the onset of the collapse of the PDEGMA brushes that is related to the local segment density near the underlying substrate would be shifted to lower temperature. The LCST could be also further optimized via copolymerization of DEGMA with, e.g., OEGMA (increase in LCST).[23] In view of potential applications, it is desirable to achieve a much more narrow LCST transition to achieve a much more pronounced difference of release rates. In particular the passive release in the low temperature state should be zero, which would be assisted reduced sorption of dye in the brush in the swollen state.

As shown above, the release rate of levofloxacin was increased ninefold by applying a thermal trigger. In addition, the bottle-shape of the pSi films enabled the loading of a high amount of drug. However, for the low molar mass dye molecule applied here, it was not possible to completely hinder the diffusion out of the pores in the "closed"-state (at low temperature). Hence, it would be necessary to apply larger carriers for the antimicrobial dye, such as polymer-dye conjugates or nanoparticles.

4. Conclusions

Bottle-shaped pSi was modified with biocompatible poly(diethylene glycol methylether methacrylate) brushes to exploit their thermoresponsiveness. PDEGMA brushes were grafted via surface-initiated atom transfer radical polymerization. The release of the fluorescent antibiotic levofloxacin, which is active against both Gram-positive and Gram-negative bacteria, from bottle-shaped pSi substrates occurred with an initial release rate that was nine times higher at 45 °C (collapsed PDEGMA) compared to 20 °C (swollen PDEGMA). Consequently, bacterial growth was strongly inhibited after thermally triggered release. It was shown in this proof of concept study that the release from pSi can be temperature-triggered after the functionalization with PDEGMA brushes. Future experiments will include long-term studies of the release to unravel the release kinetics. Further improvement of the triggered release is desirable to slow down or eliminate the release of the drug below the LCST, which can be accomplished via copolymerization with various monomers, e.g., OEGMA. Additionally, the diameter difference in the bottleneck pSi structure can be further optimized to obtain larger bottle volumes.

Supporting Information

Supporting Information is available from the Wiley Online Library or from the author.

Acknowledgements: Financial support from the EU (ERC starting grant, Grant Agreement No. 279202, Marie Curie IRSES program, Grant Agreement No. 295155, KOALA) and by the DAAD with financial support of the Bundesministerium für Bildung und Forschung, BMBF, are gratefully acknowledged. This work was performed in part at the South Australian node of the Australian National Fabrication Facility, a company established under the National Collaborative Research Infrastructure Strategy to provide nano and microfabrication facilities for Australia's researchers.

Received: March 5, 2016; Revised: April 24, 2016; Published online: ; DOI: 10.1002/macp.201600099

Keywords: atom transfer radical polymerization (ATRP); bacterial detection; porous membrane; release kinetics; stimuli-sensitive polymers

[1] K. Kirketerp-Møller, P. Ø. Jensen, M. Fazli, K. G. Madsen, J. Pedersen, C. Moser, T. Tolker-Nielsen, N. Høiby, M. Givskov, T. Bjarnsholt, *J. Clin. Microbiol.* **2008**, *46*, 2717.
[2] *Principles of Bacterial Detection: Biosensors, Recognition Receptors and Microsystems* (Ed: M. Zourob), Springer, New York **2008**.
[3] P. Goldschmidt, S. Degorge, L. Merabet, C. Chaumeil, *PLoS ONE* **2014**, *9*, e94886.
[4] a) G. Baier, A. Cavallaro, K. Vasilev, V. Mailänder, A. Musyanovych, K. Landfester, *Biomacromolecules* **2013**, *14*, 1103; b) M.-M. Sadat Ebrahimi, Y. Voss, H. Schönherr, *ACS Appl. Mater. Interfaces* **2015**, *7*, 20190; c) S. Haas, N. Hain, M. Raoufi, S. Handschuh-Wang, T. Wang, X. Jiang, H. Schönherr, *Biomacromolecules* **2015**, *16*, 832.
[5] A. Mutalib, D. Losic, N. H. Voelcker, *Prog. Mater. Sci.* **2013**, *58*, 636.
[6] a) F. S. H. Krismastuti, W. L. A. Brooks, M. J. Sweetman, B. S. Sumerlin, N. H. Voelcker, *J. Mater. Chem. B* **2014**, *2*, 3972; b) F. S. H. Krismastuti, H. Bayat, N. H. Voelcker, H. Schönherr, *Anal. Chem.* **2015**, *87*, 3856.
[7] S. J. P. McInnes, N. H. Voelcker, *Future Med. Chem.* **2009**, *1*, 1051.
[8] S. Simovic, D. Losic, K. Vasilev, *Chem. Commun.* **2010**, *46*, 1317.
[9] J. Wu, M. J. Sailor, *Adv. Funct. Mater.* **2009**, *19*, 733.
[10] S. J. P. McInnes, E. J. Szili, S. A. Al-Bataineh, J. Xu, M. E. Alf, K. K. Gleason, R. D. Short, N. H. Voelcker, *ACS Appl. Mater. Interfaces* **2012**, *4*, 3566.
[11] C. Sugnaux, L. Lavanant, H.-A. Klok, *Langmuir* **2013**, *29*, 7325.
[12] G. W. de Groot, M. G. Santonicola, K. Sugihara, T. Zambelli, E. Reimhult, J. Vörös, G. J. Vancso, *ACS Appl. Mater. Interfaces* **2013**, *5*, 1400.
[13] M. Fierheller, R. G. Sibbald, *Adv. Skin Wound Care* **2010**, *23*, 369.
[14] R. B. Vasani, S. J. P. McInnes, M. A. Cole, A. Mutalib, A. V. Ellis, N. H. Voelcker, *Langmuir* **2011**, *27*, 7843.
[15] M. Szuwarzyński, L. Zaraska, G. D. Sulka, S. Zapotoczny, *Chem. Mater.* **2013**, *25*, 514.
[16] a) H. Vihola, A. Laukkanen, L. Valtola, H. Tenhu, J. Hirvonen, *Biomaterials* **2005**, *26*, 3055; b) M. A. Cooperstein, H. E. Canavan, *Biointerphases* **2013**, *8*, 19; c) T. Takezawa, Y. Mori, K. Yoshizato, *Nat. Biotechnol.* **1990**, *8*, 854.
[17] a) A. Hucknall, S. Rangarajan, A. Chilkoti, *Adv. Mater.* **2009**, *21*, 2441; b) S. Dey, B. Kellam, M. R. Alexander, C. Alexander, F. R. A. J. Rose, *J. Mater. Chem.* **2011**, *21*, 6883.
[18] S. Desseaux, H.-A. Klok, *Biomacromolecules* **2014**, *15*, 3859.
[19] S. Han, M. Hagiwara, T. Ishizone, *Macromolecules* **2003**, *36*, 8312.
[20] E. Wassel, *PhD Thesis*, University of Siegen **2015**.
[21] E. Wassel, S. Jiang, Q. Song, S. Vogt, G. Nöll, H. Schönherr, *Langmuir* **2016**, unpublished.
[22] a) J.-F. Lutz, A. Hoth, *Macromolecules* **2006**, *39*, 893; b) X. Laloyaux, E. Fautré, T. Blin, V. Purohit, J. Leprince, T. Jouenne, A. M. Jonas, K. Glinel, *Adv. Mater.* **2010**, *22*, 5024.
[23] R. B. Vasani, D. Losic, A. Cavallaro, N. H. Voelcker, *J. Mater. Chem. B* **2015**, *3*, 4325.
[24] J. Bertino, D. Fish, *Clin. Ther.* **2000**, *22*, 798.
[25] K.-S. Tücking, V. Grützner, R. E. Unger, H. Schönherr, *Macromol. Rapid Commun.* **2015**, *36*, 1248.
[26] M. J. Sweetman, C. J. Shearer, J. G. Shapter, N. H. Voelcker, *Langmuir* **2011**, *27*, 9497.
[27] Y.-P. Kim, B. S. Lee, E. Kim, I. S. Choi, D. W. Moon, T. G. Lee, H.-S. Kim, *Anal. Chem.* **2008**, *80*, 5094.
[28] T. Higuchi, *J. Pharm. Sci.* **1963**, *52*, 1145.
[29] *Fundamentals and Applications of Controlled Release Drug Delivery* (Eds: J. Siepmann, R. A. Siegel, M. J. Rathbone), Springer, Boston, MA, US **2012**.
[30] C. Washington, *Int. J. Pharm.* **1990**, *58*, 1.
[31] a) A. Barry, P. Fuchs, F. Tenover, S. Allen, D. Hardy, J. Jorgensen, J. McLaughlin, L. Reller, *Eur. J. Clin. Microbiol. Infect. Dis.* **1994**, *13*, 822; b) R. P. Smith, A. L. Baltch, M. A. Franke, P. B. Michelsen, L. H. Bopp, *J. Antimicrob. Chemother.* **2000**, *45*, 483; c) G. P. Gesu, F. Marchetti, L. Piccoli, A. Cavallero, *Antimicrob. Agents Chemother.* **2003**, *47*, 816.